Eur J Med Chem (1995) 30, 15–25

Molecular simulation applied to 2-(*N'*-alkylidenehydrazino)- and 2-(*N'*-aralkylidenehydrazino)adenosine A_2 agonists

PP Mager*, M Richter, R Reinhardt

Institute of Pharmacology and Toxicology, University of Leipzig, 04107 Leipzig, Härtelstr, 16-18, Saxony, Germany

(Received 26 April 1994; accepted 7 September 1994)

Summary — The planar double ring system of adenine is conformationally rigid. Rotations of the ribose ring of adenosine around the *N*-glycosidic bond are hindered by nonbonded electrostatic and steric forces. The flexibility of the sugar ring and the changed conformations of the substituents of 2-(*N'*-alkylidenehydrazino)- and 2-(*N'*-aralkylidenehydrazino)adenosine A_2 agonists may be observed under changing solvent conditions and by energetic activation. Four hydrogen-bonding forces between the glutarimide rings of a recently designed pseudoreceptor and the 'pharmacophoric groups' of the adenosine derivatives may be hypothesized. Structure–activity relationships show that the A_2 agonist potency is mainly determined by the molar refraction of the substituents, the point-charge dipole moment of the molecule, and the type of substitution (aliphatic or aromatic groups).

molecular modelling / QSAR / pseudoreceptor / 2-(*N'*-alkylidenehydrazino)adenosine derivative / 2-(*N'*-aralkylidenehydrazino)adenosine derivative

Introduction

Adenosine enters cells by facilitated diffusion *via* a single, nonspecific carrier system, which is very sensitive to inhibition by adenosine derivatives. The synthetic analogs modulate neuronal function by receptor-mediated mechanisms. It was found that there are two major subtypes of receptors, called A_1 and A_2.

Roughly speaking, the major effect of the A_1 receptor is that it inhibits adenylate cyclase. In supraventricular tissue, the A_1 adenosine receptor coupled to muscarinic channels mediates negative chronotropic, dromotropic, and inotropic actions of adenosine, and an inhibitory A_1 adenosine receptor coupled to adenylate cyclase mediates the 'antiadrenergic action' of adenosine.

The A_2 receptor stimulates adenylate cyclase. The A_2 receptor can again be categorized into a ubiquitous form (A_{2b} receptors) and A_{2a}, which is predominantly localized in the brain. If the A_{2b} receptor is in the heart-circulation system, coronary vasodilation will be obtained.

While thousands of ligands selective for A_1 receptors have been developed, it is only recently that some selective A_2 agonists have been synthesized. Among them, a series of potent and selective 2-(*N'*-alkylidenehydrazino)- and 2-(*N'*-aralkylidenehydrazino)adenosine derivatives has been synthesized and tested [1, 2]. Unfortunately, the recent elucidation of the amino-acid sequence of the adenosine receptor [3] will not provide deeper insight to drug–receptor interactions because there is a lack of knowledge on the secondary and tertiary adenosine–receptor structures. Therefore, the 'superposition approach' may be used to simulate the geometry of adenosine receptor sites [4]. Another starting point for simulating certain aspects of the geometry of the adenosine receptor sites seems to be the 'scaffold approach', which allows ready assembly of receptors with high affinity for adenosine derivatives [5]. Among the number of pseudoreceptors, a newly synthesized 3,6-diaminocarbazole derivative designed by researchers at the Massachusetts Institute of Technology [5], was chosen. The reason for this choice was that the model allows us to investigate the number of hydrogen-bonding forces between the pseudoreceptor and the adenosine derivatives.

Materials and methods

Chemistry

The synthetic routes to the 2-(*N'*-alkylidenehydrazino)- and 2-(*N'*-aralkylidenehydrazino)adenosine derivatives were described elsewhere [1, 2]. The lead molecule of the two series is given in figure 1. The synthesis of the 3,6-diaminocarbazole derivative as a binding-pocket model of a pseudoreceptor was published in chart I of reference [5].

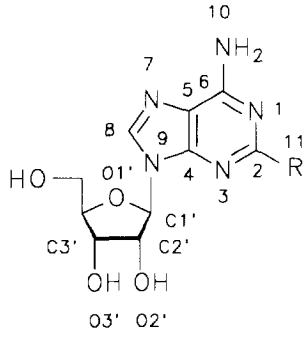

Fig 1. Structural formula (*anti* form) of adenosine and (*N*'-alkylidenehydrazino)- and 2-(*N*'-aralkylidenehydrazino)-adenosine derivatives. R = H (adenosine) or R = XX^1 where X = -NHN=CH- and X^1 = substituent.

Molecular modelling and simulation

The LFER and extrathermodynamic parameters of the substituents (fig 1) were chosen from literature [6, 7]. As many electronic and steric substituent constants were not available in table collections, only the position-independent molar refraction *MR* of the substituents was studied, together with the lipophilic substituent constant π (octanol/water). The distribution coefficient *P* (octanol/water) of the unsubstituted adenosine shows that the compound is highly hydrophilic (the experimentally measured log*P* is –1.23).

The net charges and electrostatic energies of the 2-(*N*'-alkylidenehydrazino)- and 2-(*N*'-aralkylidenehydrazino)adenosine derivatives were obtained by the semiempirical PM3 approximation [8, 9], which is a reparameterization of Austin method 1 (AM1). It is well suited for heterocyclics and intermolecular hydrogen bonds and was developed using a new optimization procedure for quickly determining atomic parameters from experimental reference data. The net charges and electrostatic energy of the 3,6-diaminocarbazole derivative were determined by the connectivity-based iterative partial equalization of orbital electronegativity (Gasteiger method), which does not depend on a particular geometry optimization [10]. In this formalism, the atomic electronegativities are not completely equalized; the atomic charges are connectivity dependent (dependent on the neighboring atoms), and residual nonzero electronegativities (difference in atomic electronegativities between the atomic electron affinities) are predicted.

Molecular mechanics (MM) calculations employed an Aufbau principle where the total energy E_{tot} is taken as the sum of local interactions found within and between separate molecular fragments. The valency interactions consisted of bond stretching and angular distortions (bond angle bending, dihedral angle torsion, and inversion terms). The nonbonded intermolecular interactions consisted of van-der-Waals (vdW) terms and electrostatic interactions, as well as special hydrogen-bonding forces.

Different molecular mechanics methods [11–18] were used to compare the results of key molecules. The MM+ force field is an improved MM2 force field with an out-of-plane bending term. It was chosen in this work as a routine method for the complete set of molecules, because it was designed for small organic molecules and expanded to amino acids, peptides, heterocyclics, and nucleic acids. Unfortunately, MM+ modules do not have an option for changing the dielectric constant ε, in contrast to AMBER 3.0 force field (assisted model building and energy refinement). If needed, the MM+ force field was used at the first phase of research, and then the AMBER 3.0 was applied to PM3-MM+ optimized conformations at the second phase of research.

The structures were refined using a conjugate gradient minimizer (Fletcher–Reeves modification of the Polak–Ribière method). Convergence was obtained when the gradient root mean square RMS was RMS < 0.01 kcal/Å•mol. Correlation-gradient geometry optimization was achieved by the following steps.

1. The conformations were initially energy minimized using force field (FF) without an electrostatic term. If not otherwise stated, we used the so-called cooling–heating–cooling schedule. After a short mechanics run (0K temperature), a fully optimized lowest-energy structure was obtained. We continued with short molecular dynamics (MD) runs (373K, 200K, 100K, 50K, and then 25K temperature) to climb the energy barriers, followed again by the usual MM minimization (0K temperature) until the procedure converged to a minimum-energy structure.
2. Molecular mechanics is not accurate enough to handle the electronic delocalization, charge-transfer effects and reactivity, and one must be particularly cautious in interpreting simulations on polar molecules if electrostatic terms are not included. Thus, the whole procedure was repeated with Coulomb's law functions (PM3 or the Gasteiger method).

After also including the electrostatic energy and repeating the cooling–heating–cooling schedule, the resulting conformation may be defined as a near-global minimum-energy conformation. Therefore, it might be hypothesized that the system 'froze' to a single crystal-like conformation.

As the molecules are polar, a distance-dependent dielectricum for different expressions of the electrostatic energy was applied under certain conditions (see above). Specifically, the following dielectric constants ε [19] were used in the AMBER 3.0 force field: ε = 1 (vacuum); ε = 3.5 (apolar environment); and ε = 80 (to approximate a hydrated molecule in aqueous solution).

Pharmacology

Details of the biological assays and the numerical data can be taken from the original study [1, 2]. The index of the A_2 adenosine receptor activity is the coronary vasodilation. The concentration ED_{50} (M) needed to get a 50% effect was obtained by logit analysis. The parameter $Y = -\log(ED_{50})$ was used in subsequent calculations to get normally distributed and variance-stabilized scores.

Mathematical and statistical analysis

The underlying statistical approach was based on the MASCA model [20, 21]. The software (IBM PCs) can be obtained by written request, together with the study guides.

Results and discussion

Adenosine: the natural outgrowth

The derivatives may be discriminated into structural moieties called core fragments. The natural outgrowth of the adenosine (R = H in fig 1) substances may be

divided into two fragments, the sugar and adenine. The logarithms of the two distribution coefficients of adenine and ribose are log$P$ = –0.09 and –2.32, but the measured log$P$ of adenosine is –1.23 (no additive behavior of lipophilicity of the two core fragments, which is an indicator of molecular interactions).

The parameters of the MM + force field are default values where no set exists. A comparison between the experimentally determined bond distances (in Å) and endocyclic bond angles (in deg) between models of the core fragments and the adenosine shows a good agreement (tables I, II). The parameters of the all-atom AMBER force field of adenine can be taken from literature, with the experimentally obtained (infrared and Raman data for polycrystalline adenine) and *ab initio* calculated vibrational frequencies, together with the structural data determined by X-ray and NMR experiments [17, 22]. The results of the two force fields agree approximately.

Table I. Comparison of two independent experimental investigations (table 29 in [17]) of purine (adenine without the exocyclic amino group) with calculated structural data (bonds in Å, angles in deg) of the adenine ring of adenosine.

*Code**	*Experimental*		*Calculated*
	1	*2*	
1-6	1.330	1.336	1.348
5-6	1.393	1.385	1.410
6-10	–	–	1.338
1-2	1.349	1.349	1.336
2-3	1.339	1.324	1.335
3-4	1.337	1.336	1.362
4-5	1.407	1.391	1.370
4-9	1.379	1.369	1.377
5-7	1.373	1.375	1.388
7-8	1.327	1.337	1.307
8-9	1.311	1.313	1.376
1-6-5	118.9	119.0	118.2
1-6-10	–	–	119.3
2-1-6	118.4	117.5	120.2
1-2-3	128.5	127.9	126.3
2-3-4	113.0	113.4	112.6
3-4-5	123.9	123.1	126.3
5-4-9	109.6	109.6	106.2
4-5-6	117.9	118.5	116.3
4-5-7	105.1	105.5	110.7
5-7-8	106.5	106.3	104.1
7-8-9	115.1	114.1	113.5
4-9-8	103.8	104.6	105.4

*See figure 1.

Table II. Comparison of an experimental investigation [26] of (*R*)-2-amino-(*s*)-4-hydroxy-(*s*)-5-methyltetrahydrofuran-(2,5-dideoxy-β-D-*erythro*-pentafuranosylamine) with calculated structural data of the ribose ring of adenosine (bonds in Å, endocyclic angles in deg).

*Atomic code**	*Experimental*	*Calculated (fig 2b)*
C1'C2'	1.517	1.530
C2'C3'	1.523	1.519
C3'C4'	1.521	1.532
C4'O1'	1.447	1.430
O1'C1'	1.420	1.427
C1'O1'C4'	109.5	111.4
C2'C1'O1'	105.8	102.7
C3'C2'C1'	101.8	100.1
C4'C3'C2'	102.1	102.8
O1'C4'C3'	106.0	104.3

*See figure 1.

The ribose ring can adopt one of the two principal puckering states: C3'-*endo* and the more stable C2'-*endo* structure (observed also in A-DNA and B-DNA, respectively). The energetic difference is about 1 kcal/mol. It agrees with the values 1.2 and 1.63 kcal/mol of HF/6-31G* and MP2/6-31G* calculations [26].

The distance of the atoms O1' atom of the sugar and the C8 atom of adenine is 2.88 Å. This nearly agrees with the sum of the oxygen and carbon van-der-Waals radii (1.52 plus 1.30 Å). The sp^2 C8 atom does not have a positive charge (–0.066 obtained by the Gasteiger method; –0.217 obtained by PM3). This implies that it cannot form electrostatic nonbonded interactions with the negatively charged O1' atom (–0.332 by the Gasteiger method; –0.255 by PM3). To bring the O1' atom *cis* (0°) to an atom in the 8-position, the C8 carbon atom must be replaced by positively charged atoms (such as divalent sulfur or selenium [28]). On the other hand, nonbonded electrostatic *repulsive* interactions between the N3 (–0.240 by the Gasteiger method; –0.142 by PM3) atom of adenine and the O1' atom of the ribose must be hypothesized. To study the repulsive electrostatic 'adenine–sugar interaction', the *N*-glycosidic torsional bond was rotated under vacuum conditions (ε = 1). It should be noted that angles of conformation analyses here are in MOBY units (not expressed explicitly in IUPAC units). The electrostatic energy was determined and added to the other energies (fig 2a). The 'global minimum' energy structure at 34.51 kcal/mol and 332° corresponds to the *anti* form (fig 2b). The subsequent values of the ordered energy levels are

34.56 kcal/mol and 689° (conformation similar to that of fig 2b). The 'first local minimum' conformation was found by an approximate 180° rotation around the *N*-glycosidic torsion angle (3° angle increment, 10 time steps), we obtained 35.42 kcal/mol at 506° (*cis* form, fig 2c). The approximate energy difference between the *anti* and *cis* form is less than ΔE = 1 kcal/mol (0.91). The frequency histogram (fig 2d) indicates that the majority of the energy states lies within the 'minimum-energy range'.

It might be expected that a change of solvent conditions may influence the energetic differences. To test this suggestion, the procedure was repeated under lipophilic (ε = 3.5) and hydrophilic environmental

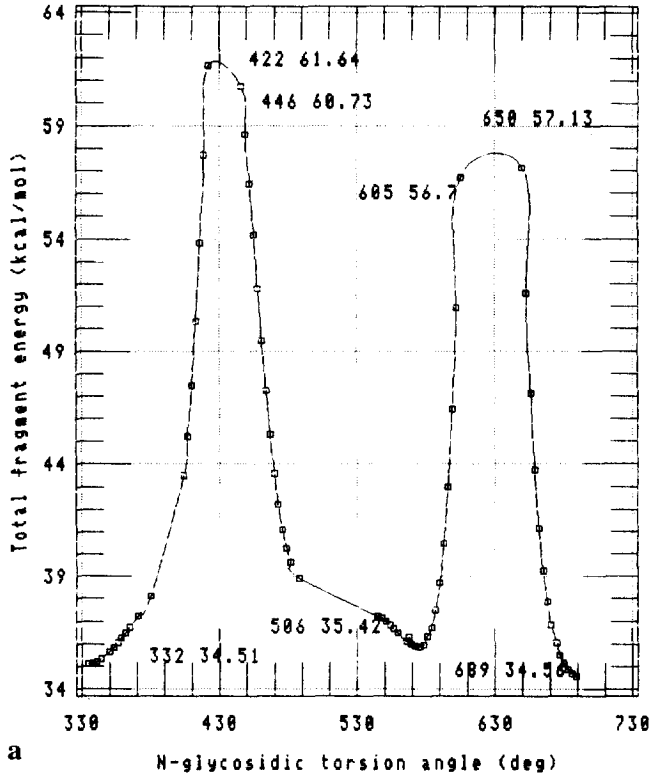

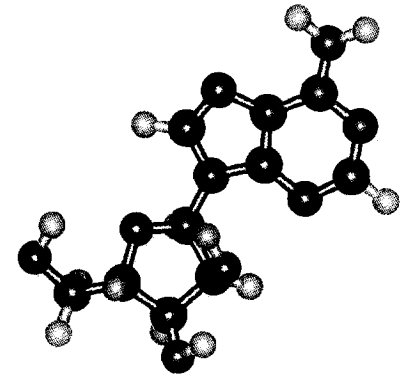

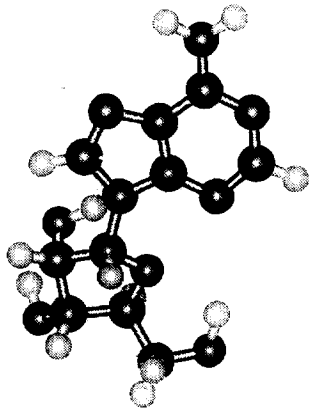

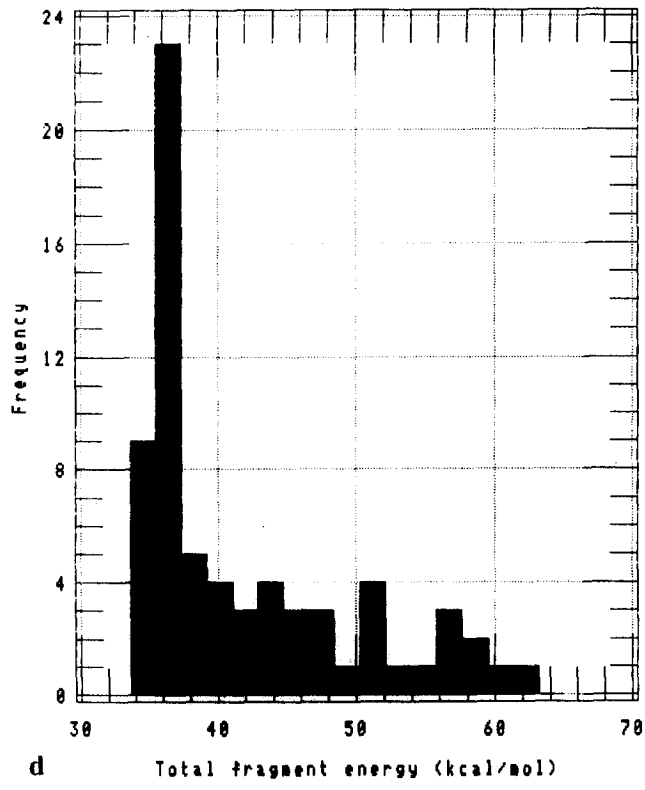

Fig 2. a. Total fragment energy of adenosine in dependence on the *N*-glycoside torsion angle. **b.** Energy-minimized *anti* conformation of adenosine. **c.** Energy-minimized *cis* conformation of adenosine. **d.** Frequency histogram of the total energy (sum of valency, nonvalency and electrostatic terms) of adenosine.

conditions (ε = 80). The total energy of *anti* form becomes 49.16 (ε = 3.5) and 54.92 kcal/mol (ε = 80). The total energy of *cis* form becomes 49.40 (ε = 3.5) and 54.99 kcal/mol (ε = 80). This gives ΔE = 0.24 (ε = 3.5) and 0.07 kcal/mol (ε = 80). Therefore, the energetic differences decrease slowly with the tendency to hydrate the molecule because the H bond moves in a larger domain with a higher degree of order [29]. Indeed, rotation of the *N*-glycosidic torsion bond at ε = 80 leads again to a bimodal curve type but the 'first local minimum' conformation after an approximate 180° rotation occurred after five time steps if ε = 80 (500°, 54.97 kcal/mol). A change of the sugar conformation in dependence on simulated solvent conditions was also reported in literature (simulated for glucose [23], and for the sugar residues of 2',3'-dideoxypyrimidines [27] and deoxadenosine [22]).

Under vacuum conditions and 0K, adenosine has a quasicrystalline lattice structure. After energetic activation, this order gets lost to some extent. The molecular dynamics module of various molecular modelling software is now applied to study the conformational changes of the lowest-energy structure of adenosine after energetic activation. A lipophilic environment (ε = 3.5) is assumed. As described [31, 32], we use a temperature change of 100K for a simulation of conditions needed to get a fairly high-energy domain of activated complexes. The resulting conformation is given in figure 3. The potential energy was equal to E = 91.48 kcal/mol. The conformation of the planar adenine ring is not largely changed. However, the exocyclic and even endocyclic bond distances and angles of the sugar are significantly changed.

Therefore, an unpredictable component in adenosine are the different interconversion states of the sugar moiety. Using Raman spectra of ribosyl C(1')-deuterated purine nucleosides, it was also found that the conformational sensitivity of adenosine actually arises from ribose ring puckering and *N*-glycosidic bond orientation [38]. A further unpredictable component is the heavy exocyclic in-plane bending amino group of the adenine ring because hydrogen-bonding forces with water must be envisaged.

The steric influence of the interconversions of sugar on the N3 atom of adenine would explain an inherent drawback associated with certain nucleosides, the inactivation of the drugs by the adenosine deaminase. It was suggested that a hydrogen bond between this N3 of the purine and Gly^{184} of the enzyme is a key factor in holding the analogs in position at the active site and enhancing catalysis during deamination [24]. It is clear that adenosine deaminase inhibitors might modify the action of A_2 agonists. Unfortunately, simple removal of this nitrogen (such as 3-deaza-) leads to a lack of A_2 antagonist *and* agonist activity. Furthermore, intracellular phosphorylation to the 5'-triphosphate form seems to be necessary to obtain active agents. This phosphorylation rate may be influenced by the sugar conformation, which itself depends on potential substituents [27]. Therefore, electronegative groups in the 3'-position may lead to an increase of the N3-O1' electrostatic repulsion, and bulky groups in 3-position may lead to a decreased metabolic N3-oxidation.

To test a new version of a program (GAMESS), which includes *ab initio* and semiempirical approaches, cyclic adenosine monophosphate was also used. With respect to nucleosides, two graphics of PM3 optimized conformations were presented (fig 4 in [37]); the *N*-glycosidic torsional angle appears to be equivalent to that shown in figure 2b.

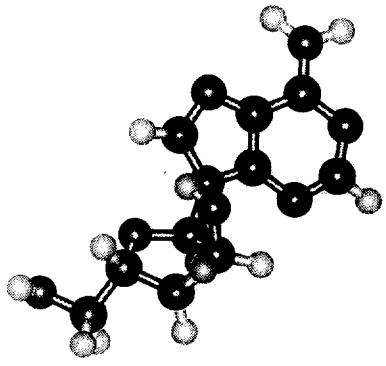

Fig 3. Conformation of the *anti* conformation of adenosine after energetic simulation (100°C) at ε = 3.5 (lipophilic environment).

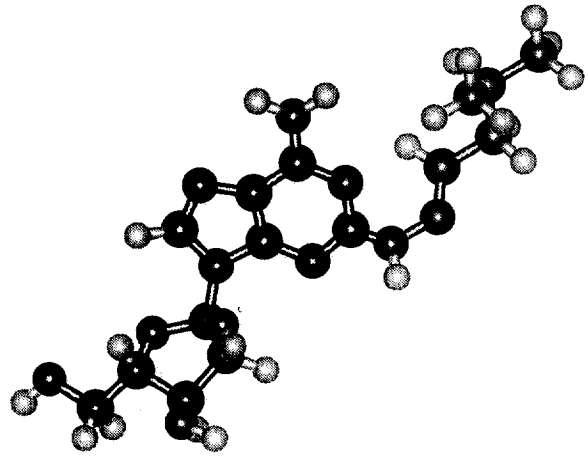

Fig 4. Conformation of compound **30** (*anti* conformation) at ε = 3.5 and 0K.

Synthetic derivatives

The drugs may be defined as adenosine, which is linked with the substituents X^1 by a short spacer, a -NHN=CH- bridge (-X- in fig 1). Compounds with related bridges such as -NHN=C(Me)- and -NHN=C(Et)- were not considered here. The -NHN=CH- bridge is less lipophilic than the linear -C≡C- bridge of other potent A_2 agonists (QSARs and molecular modelling of these agents were quite recently described [25]). The role of the -NHN=CH- bridge was studied by using the unsubstituted agent (compound **1** in table III). Rotation of the side chain is done to get the energy-minimum conformation. It was the outgrowth to obtain the substituted derivatives. Relatively complicated groups such as 7,7-dimethyl-bicyclo[3.1.1]hept-2-en-3-yl, or 4-substituted 2-thienyl, were not included in the analysis.

The first question to be answered was the influence of the substituents on the PM3-MM+ energy-minimum conformation of the substituted derivatives. A typical result of the conformation of the substituted compounds (ε = 3.5) is illustrated in figure 4 (*iso*-butyl-substituted substance). In a unidirectional orientation, it appears that the N1 nitrogen atom of the adenine ring is sterically protected by the bulky substituent.

In this series, the compounds may be classified into agents with aliphatic and aromatic substituents. To discriminate these two classes, an indicator variable X_D was introduced. Unfortunately, only a limited number of linear free-energy related (LFER) and extrathermodynamic parameters is available from table collections [6, 7]: the molar refraction *MR* and the lipophilic substituent constant π (octanol/water). Therefore, the traditional Hansch approach [6, 7] or its multivariate generalization [20, 21] cannot simply be employed to develop quantitative structure–activity relationships (QSARs), and additional parameters must be determined by molecular modelling, such as the point-charge dipole moments μ (in Debyes), various energy parameters, superdelocalizability indices, *etc*. However, it is our view that the combination of molecular modelling with multiple regression give poorer results in predicting novel agents than the traditional Hansch method. The situation may be changed in the near future because methodologies of the calculation of various parameters by quantum chemistry are available [33–36].

The following variables were listed in the design matrix: the scaled molar refraction *MR*/10, the point-charge dipole moment μ, and the indicator variable X_D (table IV). We get:

$$Y = 8.10 + 0.49\ MR/10 - 0.26\ \mu - 0.73\ X_D$$

with a multiple correlation coefficient $R = 0.66$ (the critical quantile which is based on the largest-root criterion is 0.25 at the 5% significance level). The test statistics of the regression coefficients are $t_1 = 4.20$, $t_2 = 2.02$, $t_3 = 3.47$. There are two high-leverage points (compounds **21**, **28**), two outliers (compounds **14** and **30**) but no influential point (likelihood-function distance criterion). There is no remarkable multicolinearity. The QSAR equation shows that the A_2 agonist activity is enhanced by aliphatic, bulky substituents with low dipole moments. It was surprising that the lipophilic substituent constant π (octanol/water) was insignificant.

Compound **30** has the highest A_2 agonist activity. In figure 4, the conformation was given under idealized environmental conditions (in vacuum, 0K

Table III. Substituents and biological activity.

Compound	*Substituent* X^1	*Y*
1	H	7.10
2	Ph	8.64
3	CH_2Ph	8.04
4	CH_2CH_2Ph	8.71
5	Ph-2-F	8.43
6	Ph-3-F	8.47
7	Ph-4-F	8.61
8	Ph-2-Cl	8.12
9	Ph-3-Cl	8.34
10	Ph-4-Cl	8.35
11	Ph-2-Me	7.92
12	Ph-3-Me	8.36
13	Ph-4-Me	8.49
14	Ph-2-OMe	4.91
15	Ph-3-OMe	7.91
16	Ph-4-OMe	8.76
17	2-Pyridyl	8.24
18	3-Pyridyl	7.83
19	4-Pyridyl	7.96
20	2-Thienyl	7.86
21	3-Thienyl	7.81
22	Me	7.12
23	Et	7.88
24	*n*-Pr	8.54
25	*n*-Bu	8.99
26	*c*-Hex	8.59
27	CH_2-*c*-Hex	9.16
28	CH_2CH_2-*c*-Hex	8.75
29	*iso*-Pr	8.13
30	*iso*-Bu	9.33
31	$CHEt_2$	8.24

Table IV. Physicochemical descriptors.

Compound	*MR/10*	*μ*	X_D
1	0.10	2.48	0.00
2	2.54	2.19	1.00
3	3.00	2.77	0.00
4	3.46	2.53	0.00
5	2.63	1.70	1.00
6	2.63	0.68	1.00
7	2.63	1.80	1.00
8	3.04	1.61	1.00
9	3.04	1.37	1.00
10	3.04	1.75	1.00
11	3.00	2.41	1.00
12	3.00	2.52	1.00
13	3.00	2.50	1.00
14	3.17	3.48	1.00
15	3.17	2.34	1.00
16	3.17	2.42	1.00
17	2.30	1.71	1.00
18	2.30	1.39	1.00
19	2.30	1.52	1.00
20	2.04	1.55	1.00
21	2.04	4.22	1.00
22	0.57	2.54	0.00
23	1.03	2.51	0.00
24	1.50	2.49	0.00
25	1.96	2.46	0.00
26	2.67	2.68	0.00
27	3.13	2.56	0.00
28	3.59	2.75	0.00
29	1.50	2.62	0.00
30	1.96	2.52	0.00
31	2.42	2.64	0.00

temperature). This quasicrystalline state is kinetically inactive; the drug cannot interact with its receptor or with enzymes without energetic activation. To surmount the energy-barrier height during the formation of the short-lived transition state of the drug–receptor complex, the ligand (and probably the receptor) conformation must be in a fairly high-energy domain. Therefore, atomic vibrations of the activated complex must be induced by an input of kinetic energy. Clearly, in warm-blooded animals, the temperature is not raised to achieve the transition state of drug–receptor interactions (motions due to thermally driven forces should be excluded from the considerations), and the energy for the activated complex, conversions of chemical energy into mechanical work, *etc*, comes from biochemical pathways. In simulation experiments, a rapid and strong energy increase comes from heating the molecule over, say, 3500 time steps (3.5 ps) and by 100K temperature, which usually produces productive atomic vibrations and collisions.

Table V shows the relative fragment energies during the conformational change of the unperturbed molecule (fig 4) to the energetically activated state (fig 5). Now, the N1 atom of the adenine ring (net charge –0.237) can react with electrophilic groups of the catalytic and/or accessory receptor sites. The net charge of the N3 nitrogen ring atom is –0.203; it can react with the Gly^{184} of the adenosine deaminase [24]. The most electrophilic atom of glycine is the carbonium ion of the carboxyl group (net charge by PM3: +0.231). The net charge of the nitrogen of the exocyclic amino group is weakly positive (0.109).

The electrostatic component of the aqueous solvation energy E_{solv} (kcal/mol) is the difference between the two Coulomb energies determined at $\varepsilon = 1$ and $\varepsilon = 80$ [44], or $\varepsilon = 3.5$ and $\varepsilon = 80$, respectively. Therefore, drug solubility in water is increased with increasing temperature. After energetic activation, the *iso*-butyl substituent of compound **30** *and* the ribosyl residue of

Table V. Fragment energies (kcal/mol) of compound **30** (maximum activity) prior and after energetic activation.

Energy	*Unperturbed state*[a]			*Activated state*[a]		
	Dielectric constants			*Dielectric constants*		
	$\varepsilon = 1$	$\varepsilon = 3.5$	$\varepsilon = 80$	$\varepsilon = 1$	$\varepsilon = 3.5$	$\varepsilon = 80$
Valency	39.07	39.07	39.07	85.83	85.83	85.83
1,4-Nonvalency	8.16	7.04	6.61	7.51	6.36	5.92
Van der Waals	–6.66	–6.61	–6.61	0.02	0.02	0.02
Coulomb	–7.26	–2.07	–0.09	–4.69	–1.34	–0.06
Hydrogen bonds	–0.22	–0.22	–0.22	–0.36	–0.36	–0.36

[a] E_{solv} (Coulomb) = –1.98 kcal/mol (unperturbed state) or –1.28 kcal/mol (activated state).

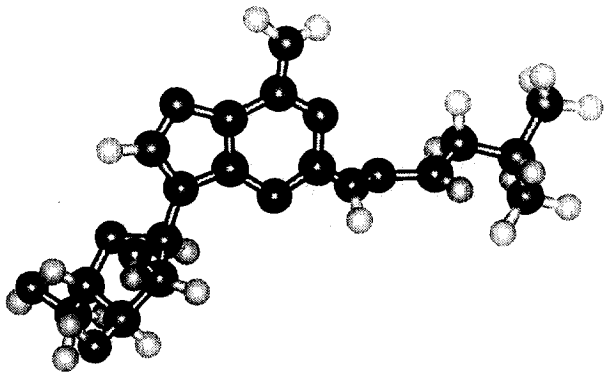

Fig 5. Conformation of compound **30** (*anti* conformation) at $\varepsilon = 3.5$ and 100°C.

the drug (fig 5) become less ordered, mainly due to the dramatic change of the valency and van-der-Waals energies in a hydrophilic ($\varepsilon = 80$) and a lipophilic environment ($\varepsilon = 3.5$). The substituent is clearly exposed to solvent. Similar effects can be observed for the other agents.

The low hydrogen-bonding energies of the neutral form of the drug *in vacuo* show that internal hydrogen-bonding forces do not play a significant role at very low and relatively high temperatures (table V). Simulating the solvent at a continuum of high (water) and low dielectric constant (lipophilic environment) does not change the situation. Although the compound may exist as ionized species at physiological pH and the calculations could have been run on the ionized forms, it might be expected that it would introduce more uncertainties than it would remove. In particular, one has to choose which charges to employ, worry about the parameterization of charges species within the force fields, and decide how to include salt effects; moreover the resulting geometries may or may not reflect the situation in solution or even at the activated receptor site. Therefore, we did not employ ionized species in geometry optimizations, and the molecules were assumed to exist as ground-state singlets.

The above results support the working hypothesis that the adenine ring is fairly rigid and acts as complementary area of the receptor site. The relative rigidity will result an enhanced selectivity. The substituents are conformationally flexible after energetic activation, and may more easily satisfy the steric requirements of the various binding centers of the A_2 receptor without steric strain because they may move between different conformations in picoseconds. The role of the conformation of the ribosyl residue is largely unpredictable under biochemical conditions.

Simulated docking: a first hypothesis

Hydrogen-bonding forces between biological receptors and drugs can be observed in experiments but pseudoreceptor–ligand interactions [5, 39] may be used for simulation experiments. Hydrogen-bonding forces between the newly synthesized 3,6-diaminocarbazole derivative [5] and the adenosine agonists might therefore be expected. Since part of the terminology concerning hydrogen-bonding forces is not uniformly used, we regard any interaction X-H...Y (H carries a positive and Y a negative charge, the charge on X is more negative than on H; and the angle at H must be $\geq 90°$) as a potential hydrogen-bonding force [29–31]. After strong energetic simulation, the bond must be disrupted. As an example of the adenine derivatives, compound **30** (largest biological activity) is used.

The Gasteiger-MM+ optimized conformation of the pseudoreceptor is used as a starting conformation. Successive rotations of the torsional angles in dependence on the energy-minimum states were then made, and the AMBER 3.0 force field was employed ($\varepsilon = 3.5$). Figure 6 illustrates this result. The energy-minimized conformation is rather resistant to environmental conditions (changes of ε and small changes in temperature).

To position certain residues of compound **30** (maximum activity) with certain residues of the pseudoreceptor in a way that they can interact with the eventual docking-targeted bonds of the drug, it must be taken into account that the different ways of putting the two molecules together tend to be infinite. In general, automatic docking is proposed, which may be regarded as computerized manual-docking process [40–42]. We used here chargeless and dimensionless 'dummy atoms', which only create vector mapping, and attempted to find the complementary areas between the drug and pseudoreceptor. Initially, a distance of 8 Å was used. The minimum energy of the complex, the distances, and angles were calculated until the data were 'physically acceptable' [43]. The dummies were then omitted again. Figure 7 shows the solvation surface of the conformation of the pseudoreceptor–drug complex. The change of conformation (figs 6 and 7) may probably be explained through induced fit which was also observed in other pseudoreceptor–nucleoside complexes [5].

At least four hydrogen-bonding forces between the pseudoreceptor and these A_2 agonists must be envisaged. The exocyclic in-plane bending N6 amino group of the adenine ring lies in a pocket of the pseudoreceptor. It is therefore available for hydrogen-bonding interactions. The distances between the hydrogen atoms of the amino group and the oxygen atoms of the -CONHCO- group of the glutarimide of

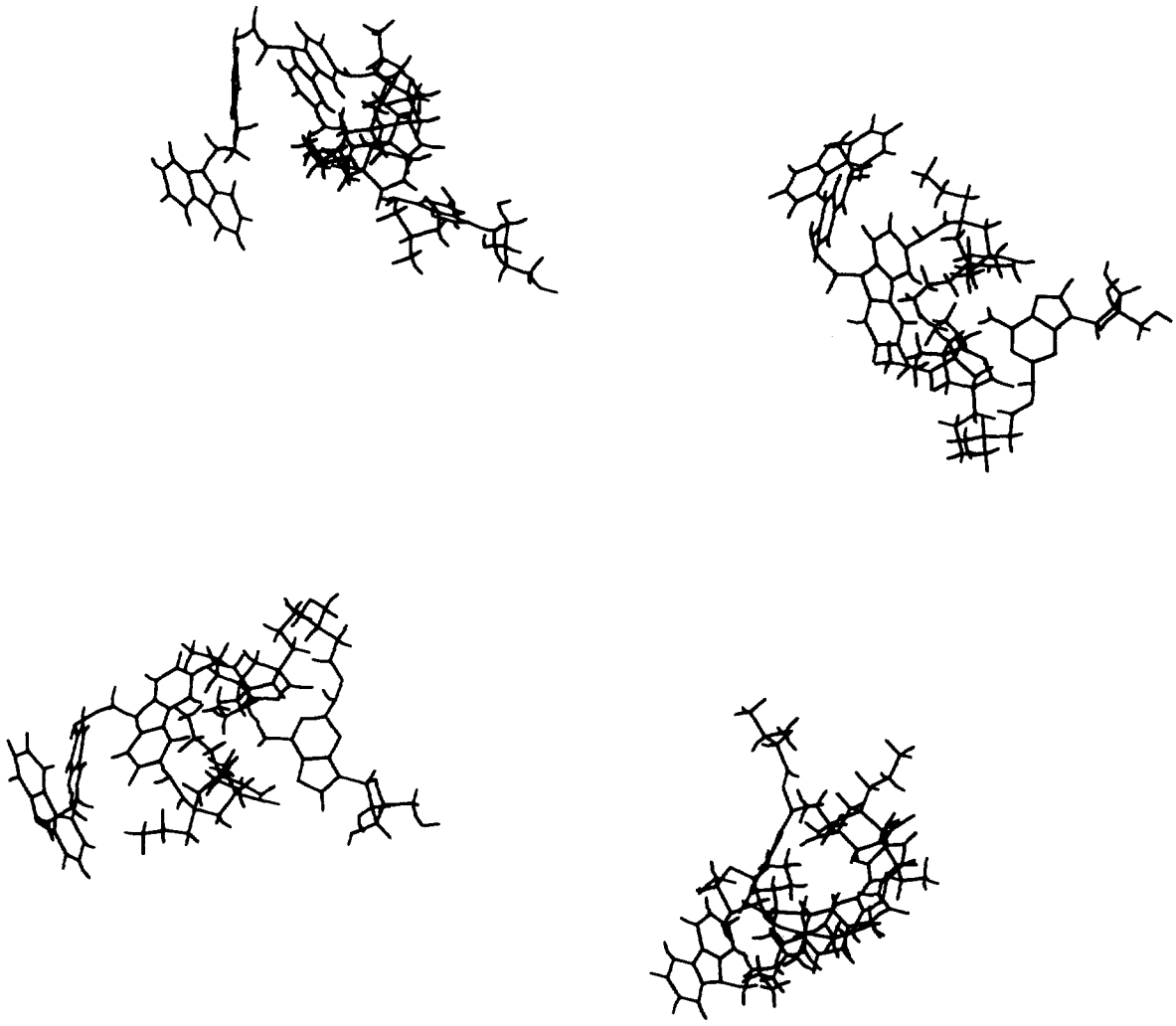

Fig 6. Portrayals of the unoccupied pseudoreceptor.

the pseudoreceptor are 2.19 and 2.18 Å, respectively. The NH...O angles are 149° and 128°, respectively. It can be visualized that substitution of a single H atom of the amino group by a bulky group is uncritical because such conformers fit into a corresponding cavity of the pseudoreceptor. However, a subjective assumption is that only NHR groups, which lower the net charge of the N atom of the amino group may increase the affinity.

The distance between the N7 atom of adenine and the hydrogen of the NH group of -CO-NH-CO- of the pseudoreceptor is 1.87 Å, the N7...H-N angle is 145°. The distance between the N1 atom of adenine and the NH group of -CO-NH-CO- of the pseudoreceptor is 2.06 Å. The N1...HN angle is 123°. It was suggested [25] that the selectivity of 2-(cycloalkylalkynyl)-adenosine derivatives is also based on a steric hindrance of this N1 atom. Furthermore, X-ray crystallographic analysis of human erythrocytic PNP–ligand complexes (PNP, purine nucleoside phosphorylase) revealed hydrogen-bonding interactions with the N1 and N7 of purine [45].

It was attempted to quantify the partial energies of H-bonding interactions [31, 46, 47]. As several factors are involved, more studies are needed. One factor is the type of the H-bond but another is the entropy because highly complex systems show a more substantial increase as simple guest–host systems.

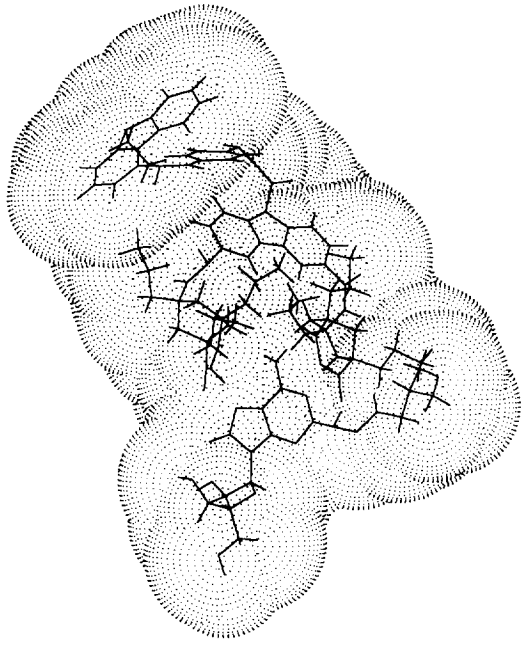

Fig 7. Solvation surface of the occupied pseudoreceptor (as a representative example, the *anti* form of compound **30** is used as a ligand).

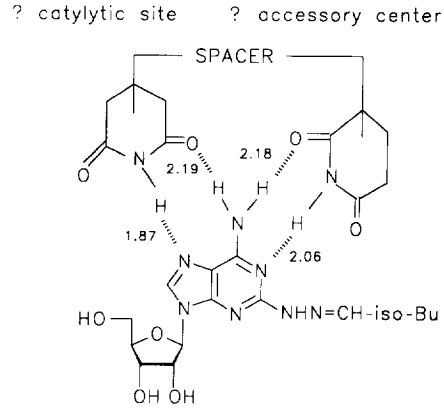

Fig 8. 'Host–guest portrayal': the distances are given in Å units. The distance between the nitrogen atoms of the two glutarimide molecules is 5.69 Å after an induced fit by a ligand. Bulky substituents which influence the point-charge dipole moment (and the net charge of the nitrogen of the exocyclic amino group?) may be involved in interactions with the accessory binding center. The role of the conformation of the ribosyl residue is largely unpredictable by this model.

The carbazole cap moved away from the adenine (driving forces for aromatic stacking in the lipophilic environment).

The host–guest recognition through the lock-and-key mechanism may be simplified for more clarity. The 2 glutarimide molecules of the pseudoreceptor are 'isolated', and a ligand is docked (fig 8). The substituents are probably involved in interactions with the unknown accessory binding center of the receptor cavity, that is, the substituents may contribute to the biological selectivity.

Needless to say that this pseudoreceptor model [5, 48] can be replaced by other models such as by aminocyclodextrins, which may also serve as a potential basis for recognition of adenosines and nucleotides in water [49]. In all cases, the models may simulate the 'biochemical reality' in certain aspects (such as hydrogen-bonding forces) but not for the whole system.

Conclusions

The planar double ring system of adenine is conformationally rigid. The flexibility of the sugar ring and changed conformations of the substituents may be observed under changing environmental conditions (energetic activation, influence of solvents). Rotations of the ribose ring of adenosine around the *N*-glycosidic bond torsion angle are hindered by nonbonded electrostatic and steric forces. The A_2 agonist affinity is mainly determined by the molar refraction of the substituents, the point-charge dipole moment, and the type of aliphatic/aromatic substitution. Four hydrogen-bonding interactions between the glutarimide rings of a recently designed pseudoreceptor and the pharmacophoric groups of adenine derivatives (N1, N7, exocyclic amino group) may be hypothesized.

References

1 Niiya K, Olsson RA, Thompson RD, Silvia SK, Ueeda M (1992) *J Med Chem* 35, 4557–4561
2 Niiya K, Thompson RD, Silvia SK, Olsson RA (1992) *J Med Chem* 35, 4562–4566
3 Libert F, Parmentier M, Lefort A *et al* (1989) *Science* 244, 569–572
4 Van der Wenden EM, IJerman AP, Soudijn W (1992) *J Med Chem* 35, 629–635
5 Conn MM, Deslongchamps G, de Mendoza J, Rebek Jr J (1993) *J Am Chem Soc* 115, 3548–3557
6 Hansch C, Leo A (1979) *Substituent Constants for Correlation Analysis in Chemistry and Biology*, Wiley, New York, USA
7 Hansch C (1971) Quantitative Structure–Activity Relationships. *In: Drug Design* (Ariëns, ed), Academic Press, New York, USA, Vol I, 271–342
8 Aleman C, Lugue FJ, Orozco M (1993) *J Comput Chem* 7, 799–808
9 Jurema MW, Shields GC (1993) *J Comput Chem* 14, 89–104
10 Gasteiger J, Marsili M (1980) *Tetrahedron* 36, 3219–3288
11 Weiner SJ, Kollman PA, Case DA *et al* (1984) *J Am Chem Soc* 106, 765–784
12 Weiner SJ, Kollman PA, Nguyen DT, Case DA (1986) *J Comput Chem* 7, 230–252
13 Momany FA, Rone R (1992) *J Comput Chem* 13, 888–900

14 Allinger NL (1987) MM2(87) Force Field. TRIPOS Associates, Inc. Saint Louis, MO. USA
15 Allinger NL, Zhu Z, Vhen K (1992) *J Am Chem Soc* 114, 6120–6133
16 Allinger NL, Yan L (1993) *J Am Chem Soc* 115, 11918–11925
17 Tai JC, Yang L, Allinger NL (1993) *J Am Chem Soc* 115, 11906–11917
18 SYBYL/ALCHEMY III package. TRIPOS Associates, Inc. Saint Louis, MO, USA
19 Bladergroen W (1949) *Physikalische Chemie in Medizin und Biologie*. Wepf & Co, Verlag, Basel, Switzerland, 189
20 Mager PP (1975) *Drug Res* 25, 1006–1008, 1270–1272, 1355–1356, 1475–1476, 1745, 1864–1865
21 Mager PP (1991) *Design Statistics in Pharmacochemistry*. Wiley & Research Studies Press Ltd, New York, USA
22 Wunz TP (1992) *J Comput Chem* 13, 667–673
23 Kouwijzer MLCE, Van Eijck BP, Kroes SJ, Kroon J (1993) *J Comput Chem* 14, 1281–1289
24 Wilson DK, Rudolph FB, Quiocho FA (1991) *Science* 252, 1278–1284
25 Mager PP (1994) *Eur J Med Chem* 29, 369–380
26 Miaskiewicz K, Osman R (1994) *J Am Chem Soc* 116, 232–238
27 Everaert DH, De Ranter CJ (1993) *J Am Chem Soc* 115, 11209–11212
28 Burling FT, Goldstein BM (1992) *J Am Chem Soc* 114, 2313–2320
29 Ruelle P, Buchmann M, Nam-Tran H, Kesselring UW (1992) *J Comput Aid Mol Design* 6, 431–448
30 Steiner T, Saenger W (1993) *J Am Chem Soc* 115, 4540–1088
31 Mager PP (1994) *Med Res Rev (New York)* 14, 75–126
32 Mager PP, Mager H, Walther H (1993) *Drug Design & Discovery (Lond)* 10, 135–156
33 Van de Waterbeemd H (1993) *Drug Design & Discovery (Lond)* 9, 277–285
34 Cramer CJ, Famini GF, Lowrey AH (1993) *Acc Chem Res* 26, 599–605
35 Famini GR (1989) *Using Theoretical Descriptors in Structure Activity Relationships*. US Army Chemical Research, Development, and Engineering Center, Aberdeen Proving Ground, MD, USA
36 Bareman JP, Reid RI, Hrymak AN, Kavassalis TA (1993) *J Mol Simul* 11, 243–250
37 Schmidt MW, Baldridge KK, Boatz JA *et al* (1993) *J Comput Chem* 14, 1347–1363
38 Toyama A, Takino Y, Takeuchi H, Harada I (1993) *J Am Chem Soc* 115, 11092–11098
39 Hung CY, Höpfner T, Thummel RP (1993) *J Am Chem Soc* 115, 12601–12602
40 Meng EC, Shoichet BK, Kuntz ID (1992) *J Comput Chem* 13, 505–524
41 Leach AR, Kuntz ID (1992) *J Comput Chem* 13, 730–748
42 Shoichet BK, Bodian DL, Kuntz ID (1992) *J Comput Chem* 13, 380–397
43 Bohacek RS, McMartin C (1992) *J Med Chem* 35, 1671–1684
44 Murukami Y, Kikuchi J, Ohno T *et al* (1991) *J Am Chem Soc* 113, 8229–8242
45 Ealick S, Rule SA, Carter DC *et al* (1990) *J Biol Chem* 265, 1812–1820
46 Vicent C, Fan E, Hamilton AD (1992) *Tetrahedron* 33, 4269
47 Schneider HJ, Juneja RK, Simova S (1989) *Chem Ber* 122, 1211
48 Kato Y, Conn M, Rebek Jr J (1994) *J Am Chem Soc* 116, 3279–3284
49 Eliseev AV, Schneider HJ (1994) *J Am Chem Soc* 116, 6081–6088